MOLECULAR PHYSICS, 1999, VOL. 97, NO. 5, 611–627

Dielectric relaxation of β-cyclodextrin complex with 4-*t*-butylbenzyl alcohol

JOHN C. PAPAIOANNOU[1]*, NIKOS D. PAPADIMITROPOULOS[1] and IRENE M. MAVRIDIS[2]

[1] Department of Chemistry, Laboratory of Physical Chemistry, University of Athens, P.O. BOX 64004, 157 10 Zografou, Athens-Greece

[2] Institute of Physical Chemistry, N.C.S.R. 'Demokritos', Aghia Paraskevi, 15310, Greece

(*Received 23 March 1999; accepted 3 May 1999*)

The frequency and temperature dependence of the real (ε') and imaginary (ε'') parts of the dielectric constant of polycrystalline complex β-cyclodextrin–4-*t*-butylbenzyl alcohol [β-CD·TERB·11.2H_2O] and β-cyclodextrin [β-CD·9.8H_2O] and of the corresponding dried forms (β-CD·TERB·3.8H_2O and β-CD·2.4H_2O, respectively) has been investigated, in the frequency range 0–100 kHz and temperature range 130–350 K. The dielectric behaviour is described well by Debye-type relaxation (α dispersion). All systems except for the β-CD·TERB·3.8H_2O, exhibit an additional Ω dispersion at low frequencies, which usually is attributed to proton transport. In the non-dried samples the temperature dependence of ε' and ε''_{max} exhibits two steps, whereas in the dried samples it exhibits only the low temperature step. The low temperature step is due to the tightly bound water molecules, whereas that at higher temperatures is due to easily removable water. The temperature dependence of ε'' shows a peak which has been attributed to a transition between ordered and disordered hydroxyl β-CD groups, and water molecules. The relaxation time varies exponentially with temperature (in the range 8–12 μsec), in a reverse *V* like curve, with maximum values located at the corresponding order–disorder transition temperatures. Activation energies of the order of ~2.5 kJ mol^{-1} are calculated for the transition in every sample. The disorder in the hydrogen bonding is equivalent to a system of two dipoles with opposite directions, and the model of Fröhlich can be applied to explain the order–disorder transition and the temperature dependence of the relaxation time. An apparent negative activation energy before the transition temperature can be attributed to reorientation of the hydrogen bonding around the cyclodextrin molecules, and it is related to endothermic drifts observed by calorimetric studies of β-CD. The order–disorder transition can be probed also from the phase shift component of the current passing through the sample relative to the applied signal.

1. Introduction

X-Ray [1] and neutron [2] diffraction studies by Saenger and colleagues have shown that in the crystal structure of β-cyclodextrin (β-CD)·11H_2O some water molecules and hydroxyl groups are statistically disordered. Specifically, the eleven water molecules are distributed over 16 positions of which 3 are fully occupied. 6.13 water molecules are in the cavity distributed over 8 positions of which only one is fully occupied, 4.85 are out of the cavity in 8 interstitial sites of which 2 are fully occupied. At room temperature there are 53 hydrogen bonds per asymmetric unit. 35 of these are of the normal type O—H···O—H··· and 18 are of the type called by Saenger *et al.* 'flip-flop', O—H···H—O [3]. The H atoms located 1 Å apart are only half occupied in the flip-flop type bond due to disorder, which is related to rotation of OH groups according to the scheme:

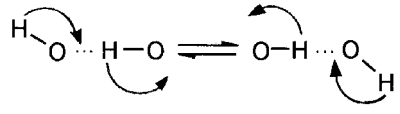

Preliminary calorimetric measurements of β-CD·11H_2O [1] in crystalline powder form showed an exothermic process at 226 K when the sample was cooled down to 100 K. The process was attributed to an ordering of dynamically disordered flip-flop H bonds into one or the other form at low temperatures. This was verified by a neutron diffraction study of β-CD·11D_2O at 120 K [4], where most of the flip-flop-type hydrogen bonds had disappeared. Hanabata *et al.*

* Author for correspondence. e-mail: jpapaio@cc.uoa.gr

Molecular Physics ISSN 0026–8976 print/ISSN 1362–3028 online
http://www.tandf.co.uk/JNLS/mph.htm
http://www.taylorandfrancis.com/JNLS/mph.htm

[5] also found an exothermic process, which started around 120 K, and became endothermic above 154 K. The sample returned to normal behaviour around 170 K and a first-order phase transition occurred at 226 K.

Consequently, calorimetric and dielectric studies of β-CD·11H_2O [6] have shown a first-order phase transition beginning at ~203 K. The plots of permittivity (ε') and loss (ε'') versus temperature showed this transition at 209.8 K, and it was attributed to the very gradual onset of proton ordering in the arrangement of water molecules with decrease in temperature. Above 250 K there is a rapid rise in ε'' with increasing temperature which is caused by the movements of protons (protonic conduction). The same behaviour has been observed in protein–water interactions [7, 8], where two kinds of water molecule have been identified. The main characteristic of the dielectric behaviour of proteins is that they exhibit two kinds of dielectric dispersion, designated Ω and α, and Ω dispersion is of biological importance because it is related to the proton transfer mechanism.

Since cyclodextrin inclusion complexes are of interest in fundamental research as well as for industrial applications, we examine in this paper the dielectric properties of the inclusion complex of β-CD with 4-*t*-butylbenzyl-alcohol (β-CD·TERB). Furthermore, we attempt a comparison of the dielectric characteristics with those of β-CD. In both cases the samples were under the same humidity (15%) at ambient temperatures.

Crystallographic studies of β-CD·11H_2O under various humidity conditions [9], have shown that it loses some crystal water reversibly (from 12.3 molecules of H_2O at 100% humidity to 9.4 at 15% humidity per β-CD molecule), but the crystalline structure remains intact.

The X-ray study of the crystal structure of β-CD·TERB·10.2H_2O [10] has shown that two β-CD molecules are held together by hydrogen bonds to form dimers in the cavity of which two 4-*t*-butylbenzyl alcohol molecules are accommodated. The interdimer space contains 10.2 water molecules, distributed over 15 sites that form a hydrogen bond network with themselves and the β-CD hydroxyl groups. The *t*-butyl groups are buried inside the hydrophobic cavity, while the polar hydroxyl groups protrude from the cavity at the primary sides of the dimer.

The role of water molecules is of fundamental importance in cyclodextrins and, as already mentioned, Ω dispersion is associated with charge carriers that hop between localized sites (protonic conduction). The mechanism of the protonic conduction, the contribution to it of water molecules inside and outside the cavity and the conditions that determine its absolute values are not clear. In the present work we investigate both dielectric dispersions (α, Ω) and the possible mechanisms that might cause them, for the systems β-CD·TERB and β-CD in the frequency range 0–100 kHz and temperature range 100–320 K. Further, we examine the dielectric relaxation results relative to the nature of the first-order phase transition by the application of Fröhlich's model to the flip-flop hydrogen bond.

2. Experimental

β-Cyclodextrin (MW 1135.01) was purchased from Fluka Chemika and was recrystallized (non-dried sample) once from water and then it was dried in the air for 5 minutes. Thermogravimetric analysis (TA Instruments 2050, heating rate 10°C min^{-1}) was used to determine the water content which was 9.8 water molecules per β-CD (β-CD·9.8H_2O), figure 1). A second sample (dried sample) was dried in an oven kept at 45°C for two days and then it was kept in a desiccator. Thermogravimetric analysis, as before, and the coulometric Karl–Fisher titration method (Metrom 652 KF-coulometer) were used to find the water content of the dried sample which was determined as 2.4 water molecules per β-CD (β-CD·2.4H_2O). The preparation of β-CD·TERB·10.2H_2O complex is described elsewhere [10]. In order to obtain dried β-CD·TERB the same experimental procedure was followed as in the case of β-cyclodextrin. The water content of the non-dried and dried β-CD·TERB complexes was determined to be 11.2 and 3.8 water molecules per complex molecule (β-CD·TERB·11.2H_2O and β-CD·TERB·3.8H_2O), respectively. Thermogravimetric analysis was used for the water content of β-CD·TERB·11.2H_2O and thermogravimetric and Karl–Fischer methods were used for the β-CD·TERB·3.8H_2O sample. Thus the dried samples of β-CD and β-CD·TERB contain 2.4 and 3.8 molecules H_2O and the non-dried contain 9.8 and 11.2 molecules H_2O, respectively. By extensive heating of the sample at 45°C the water molecules, which occupy removable sites in crystal lattice, can be distinguished from the tightly bound water molecules [11].

Pressed pellets of powdered samples, 20 mm in diameter with thickness between 0.5 mm and 2 mm were prepared with a pressure pump (Riken Power model P-1B) at room temperature. Two platinum foil electrodes were pressed at the same time with the sample. The pellet was then loaded in a temperature-controlled chamber, between two brass rods accompanied by a compression spring. A K-type thermocouple was kept close to the sample, and the whole cell was kept under an N_2 atmosphere. The humidity in the cell chamber as measured by a Digital thermo-hygrometer was 15% at room temperature at the beginning and the end of each experiment.

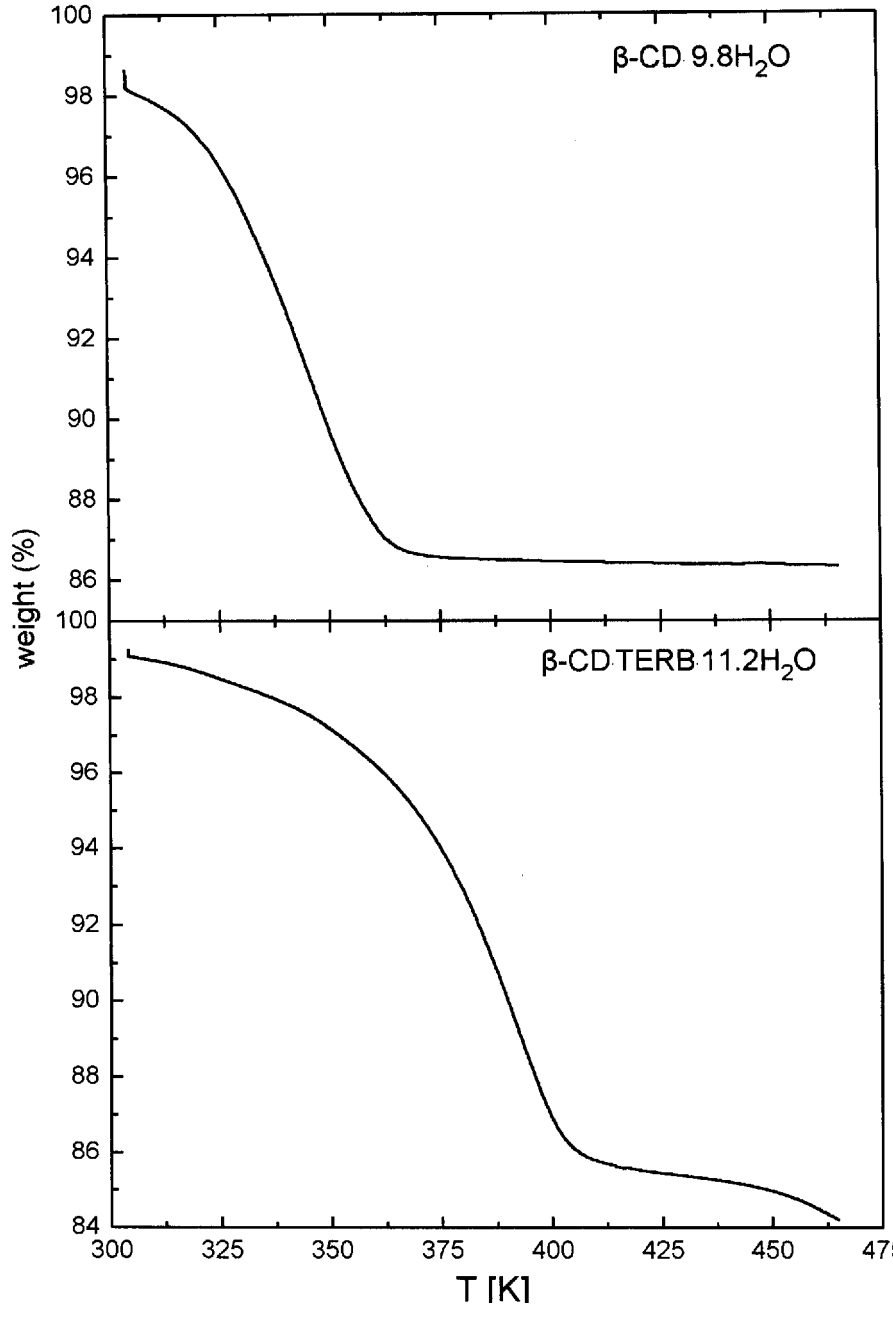

Figure 1. Thermogravimetric analysis (TGA) of non-dried β-CD·9.8H_2O and β-CD·TERB·11.2H_2O.

Impedance spectroscopy (IS) experiments utilized a Hewlett-Packard 3561A low frequency dynamic signal analyser (DSA) operating in both frequency and time domains (up to 100 kHz) which is capable of measuring amplitude and phase accurately relative to a trigger signal. The instrument can measure simultaneously the amplitude of the impedance vector and the phase shift of the sample under consideration at each frequency value in the region between 0 and 100 kHz. The data can be transferred to a PC through an HP 82335 interface bus (IEEE-488), where it can be stored and analysed by a software program [12]. The imaginary and real parts of either impedance or dielectric constant versus frequency and temperature and the Cole–Cole plots can be calculated and plotted by the program 'wplot' [13] version 1.4.

DSA applies a signal of periodic noise 72.5 mV_{rms} to the sample connected in series with a fixed known resistance $R_i = 45.6\,k\Omega$. The voltage drop across the external resistance V_i was kept at less than 10% of the applied, to minimize the effects of R_i on the phase difference. Initially the sample was short-circuited and

the amplitude spectrum (signal level as a function of frequency) and the phase spectrum (phase as a function of frequency) of the periodic noise signal across the resistance were displayed simultaneously and stored in memories M_1 and M_2 of the DSA. Thereafter, the sample was connected and the same procedure was repeated. The new amplitude and phase spectra of the signal across the resistance R_i were displayed also and stored in the buffer memory of the DSA. Then by use of the 'math function' the amplitude voltage ratio V_i/V versus frequency and the phase shift ϕ versus frequency of the corresponding traces were calculated. These data were stored in the internal non-volatile memory, where up to 40 contiguous time records could be stored for additional processing. The above data acquisition time was of the order of 4 ms for a full impedance spectrum.

It is worth noting that following the above procedure the influence of parasitic capacitance was completely obliterated, since their contribution is included in the phase spectrum which is the reference in memory M_2.

3. Results

3.1. *Frequency dependence of dielectric permittivity*

3.1.1. *Dry samples*

The frequency dependence of the real (ε') and imaginary (ε'') parts of the dielectric constant in the frequency range 0–100 kHz for fixed temperatures, during the cooling experiment from 320 K to 124 K, are shown in figure 2 for β-CD·TERB·$3.8H_2O$ and in figure 3 for β-CD·$2.4H_2O$. Every curve is composed of 800 experimental points (400 points for the 1 kHz–100 kHz range and 400 points for the 0–1 kHz range). It is observed that generally the ε' versus frequency curves are of sigmoidal shape with the inflection point at around 20 kHz. In the case of the β-CD·TERB·$3.8H_2O$, over the low frequency range 100–2000 Hz the slope of the curves increases with decreasing frequency for temperatures between 170 K and 252 K, whereas the curves are almost flat at temperatures close to 124 K and 320 K. In the case of β-CD·$2.4H_2O$ the corresponding slopes of ε' versus frequency increase with decreasing frequency for every temperature.

The frequency variation of ε'' has the form of a loss peak, centred at a characteristic frequency f_{max}. This loss peak is broad, with a half-height width of 1.18 decades of frequency. In the case of β-CD·TERB·$3.8H_2O$ only the α-dispersion is apparent. In the case of β-CD·$2.4H_2O$ both α and Ω dispersions, are observed. In both cases the α dispersions are described by the Debye relaxation type (see discussion). The ε''_{max} values of each loss peak increase with temperature from 1.3 to 3.2 for β-CD·TERB·$3.8H_2O$ and from 1.5 to 4.8 for β-CD·$2.4H_2O$ (figure 4(*a*)). The values in both samples coincide in the low temperature limit and deviate as the temperature increases. The inflection points appear at ~250 K and ~215 K for β-CD·TERB and β-CD, respectively. The accurate value of f_{max} for each curve of ε'' versus frequency was found by fitting the local maximum over a short range of frequency. The relaxation time $(\tau = 1/2\pi f_{max})$ in both cases is strongly dependent upon temperature as depicted in figure 5(*a*). The maxima of 10.3 μs for β-CD·$2.4H_2O$ and 9.8 μs for β-CD·TERB·$3.8H_2O$ occur at the transition temperatures 215 K and 250 K, respectively.

In order to test whether the low frequency dielectric dispersion Ω, in the case of β-CD·$2.4H_2O$, arises from proton conduction processes, blocking electrodes composed of Pt/mica were used to inhibit charge carrier injection into the sample. The frequency and temperature dependence of ε' and ε'' were the same as before, except for the smaller absolute values. The Ω dispersion disappeared whereas the α dispersion was unaffected. The same observations were obtained by Morgan and Pethig for various polycrystalline proteins [14, 15].

3.1.2. *Non-dry samples*

In both samples, β-CD·$9.8H_2O$ and β-CD·TERB·$11.2H_2O$, α and Ω dispersions were observed. The absolute values of ε' and ε'' in the case of β-CD·$9.8H_2O$ were found to be the same as those reported previously [6]. Our results differ in the temperature variation of frequency maxima. The resulting relaxation time exhibits the temperature variation depicted in figure 5(*b*).

The ε''_{max} versus T plot has a double-step-like form in both β-CD·$9.8H_2O$ and β-CD·TERB·$11.2H_2O$, as depicted in figure 4(*b*).

3.2. *Variation of ε' and ε'' with temperature*

3.2.1. *Dry samples*

The plots of ε' and ε'' against temperature for the fixed frequencies 200 Hz, 1 kHz, 100 kHz are shown in figures 6 and 7.

The ε' values of β-CD·TERB·$3.8H_2O$, at 200 Hz, increase in a step-like form from 2.5 at low temperatures to 6.5 at high temperatures. The corresponding values of β-CD·$2.4H_2O$ are almost the same as in β-CD·TERB·$3.8H_2O$ in the low temperature limit but at high temperatures they deviate strongly to higher values $(\Delta\varepsilon' = 4.3)$. The same qualitative picture is observed for the other, higher fixed frequencies but with smaller deviations, i.e., at 1 kHz $\Delta\varepsilon' = 3.2$ and at 100 kHz $\Delta\varepsilon' = 0.2$. The coincidence of the ε' versus T curves of the two samples over the temperature interval $T < 215$ K at a constant frequency of 100 kHz is remarkable.

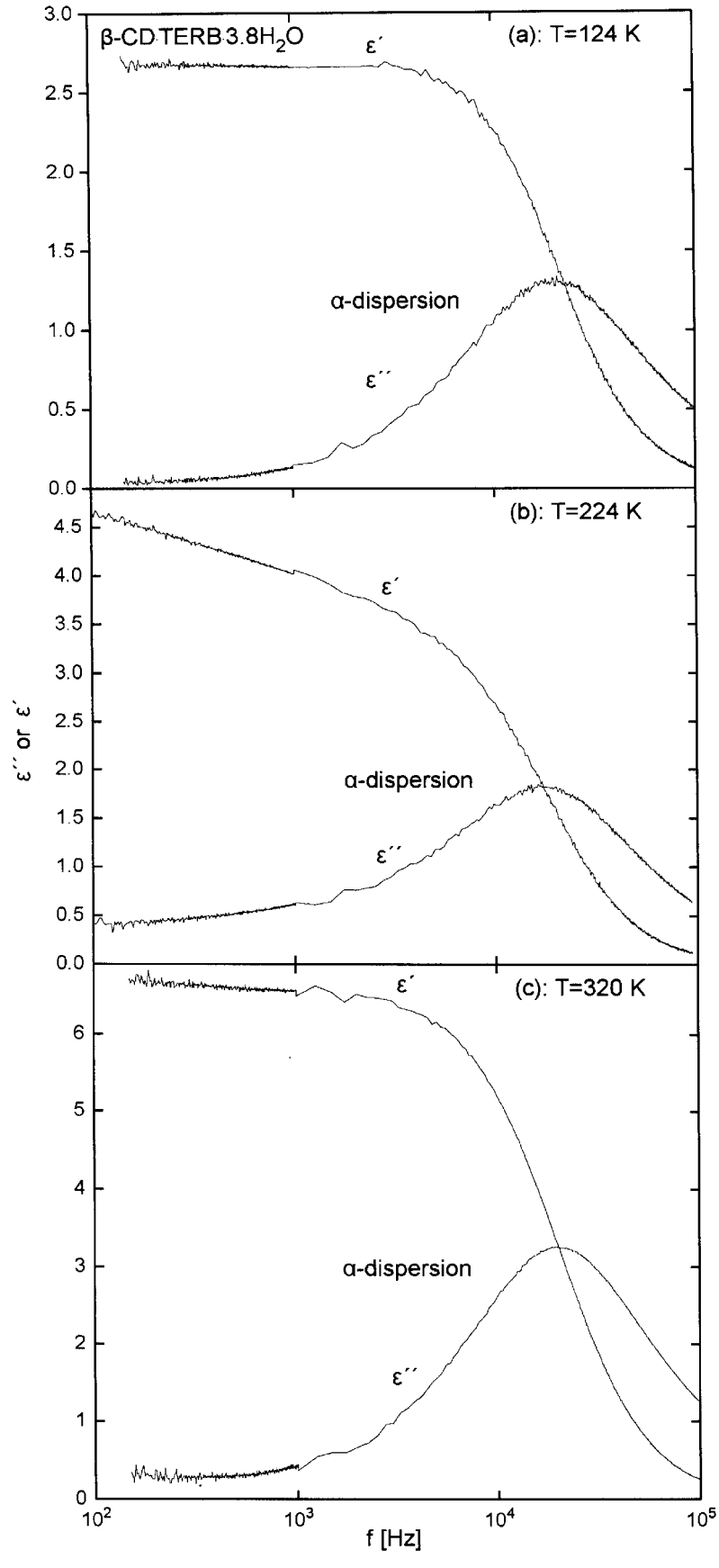

Figure 2. Frequency dependence of real (ε') and imaginary (ε'') parts of the dielectric constant of the β-CD · TERB · $3.8H_2O$ for fixed temperatures (a) 124 K, (b) 224 K and (c) 320 K.

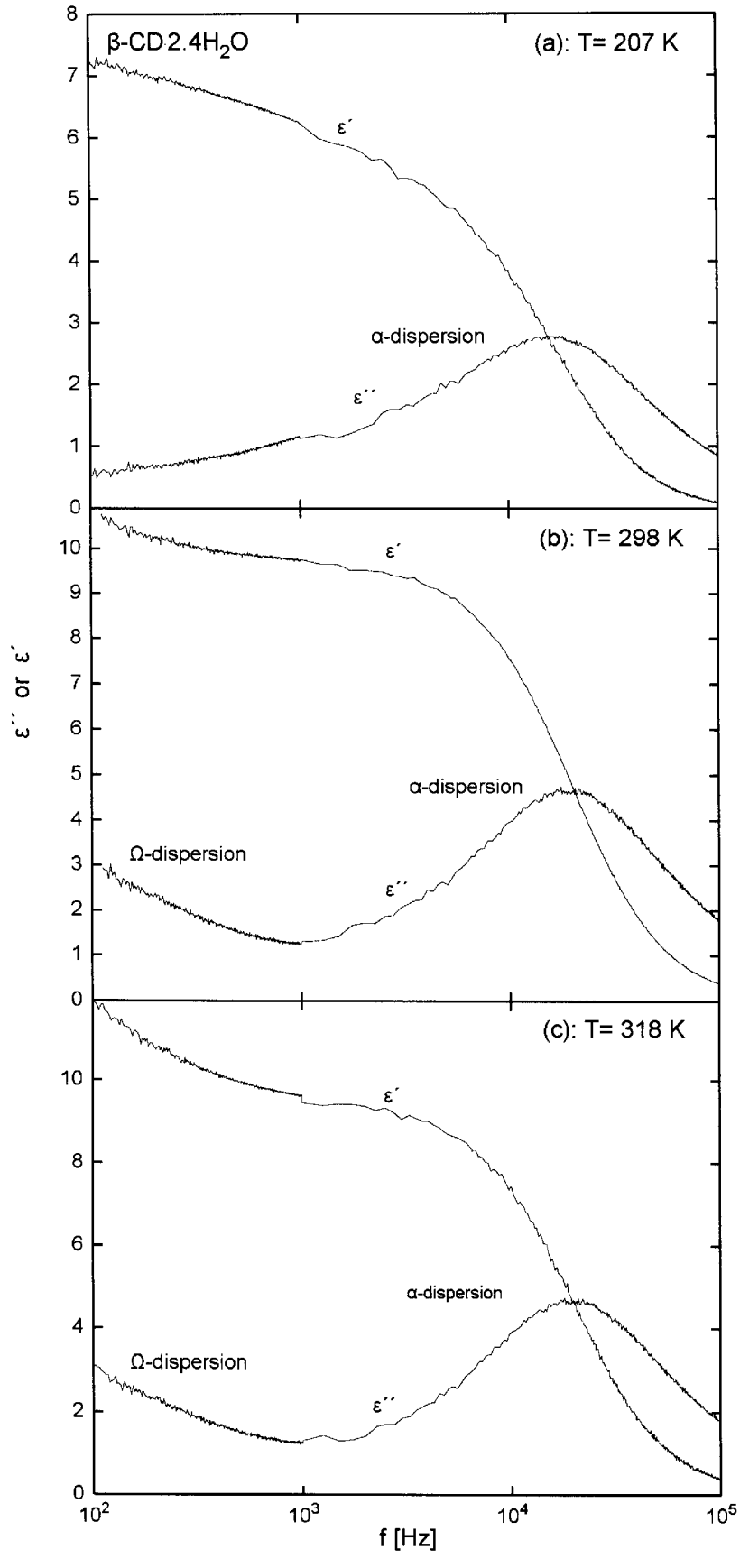

Figure 3. Frequency dependence of real (ε') and imaginary (ε'') parts of the dielectric constant of the β-CD·2.4H_2O for fixed temperatures (a) 207 K, (b) 298 K and (c) 318 K.

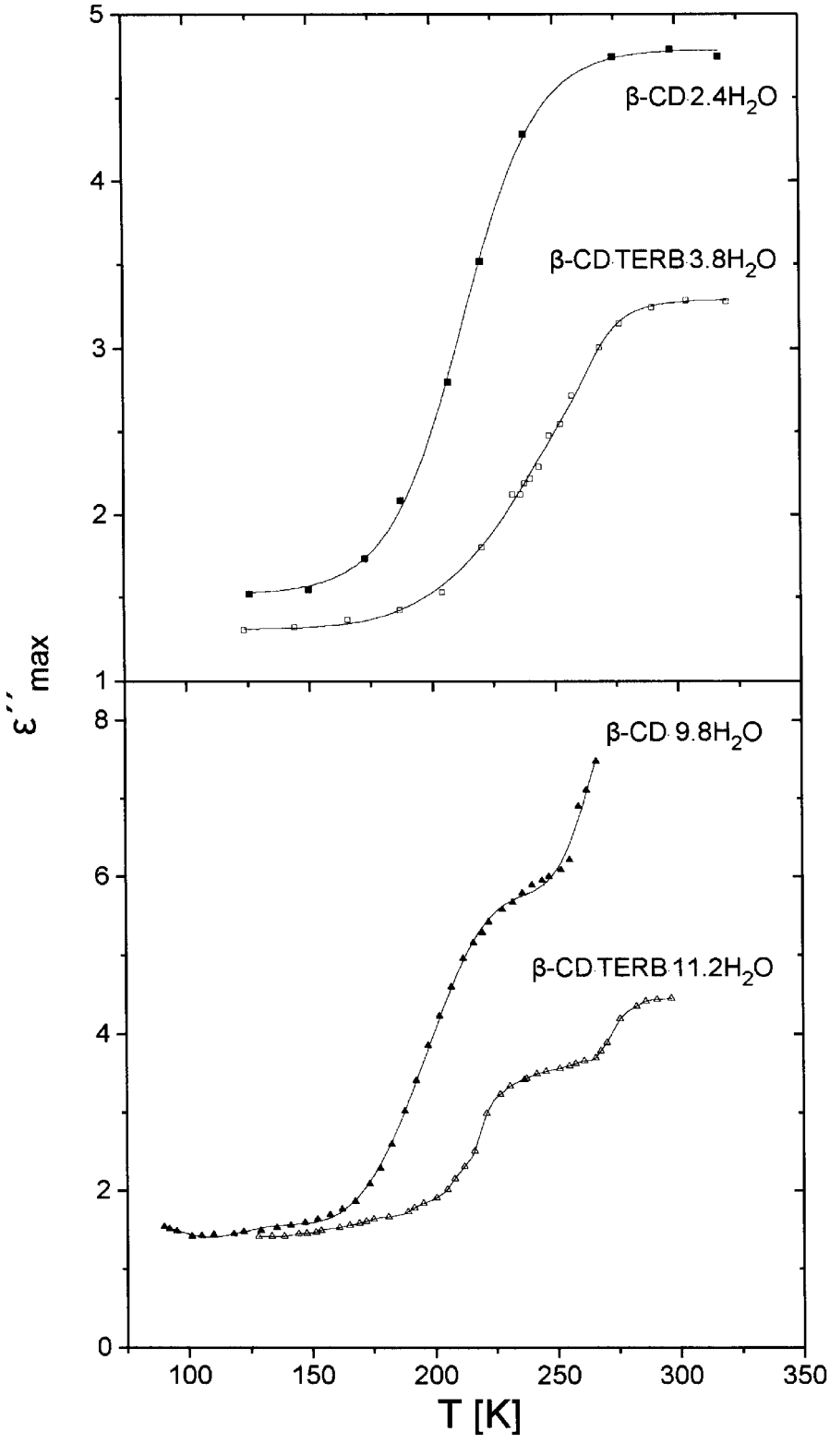

Figure 4. Plot of ε''_{max} against temperature for (*a*) dried and (*b*) non-dried samples of β-CD·TERB and β-CD.

The ε'' versus T curve of β-CD·TERB·3.8H_2O at 200 Hz is broad-bell shaped with a maximum value at 230 K and a half-width of ~150 K. This maximum absorption shifts to higher temperatures and becomes less broad by increasing the frequency up to 1 kHz. Beyond this frequency the bell-shaped ε'' versus T curves are transformed to step-like curves. In the case of dried β-CD·2.4H_2O the maximum value of ε'', at

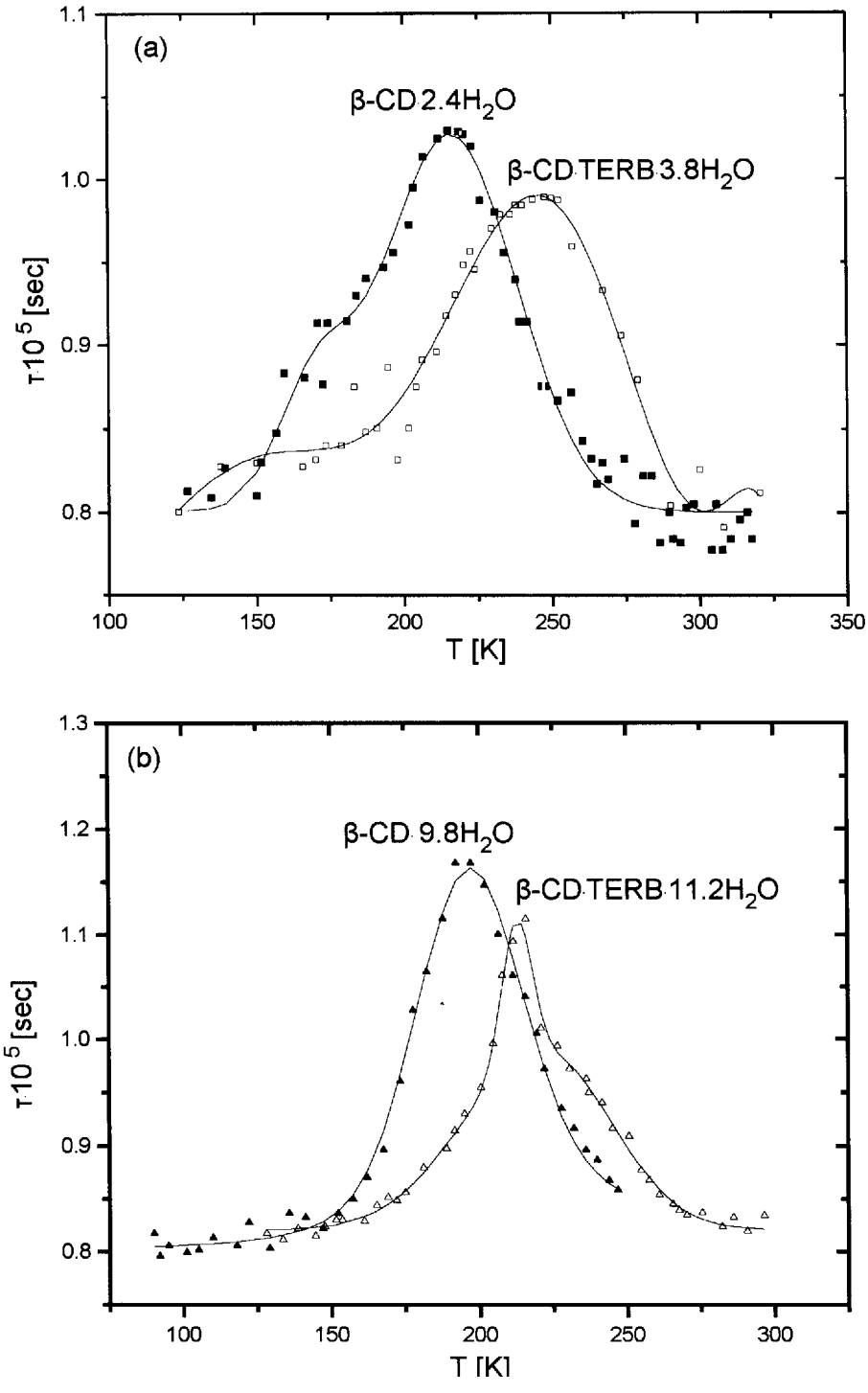

Figure 5. Relaxation time against temperature for (*a*) dried, and (*b*) non-dried samples of β-CD·TERB and β-CD.

200 Hz, is found at 196 K and shifts to higher temperatures as the frequency increases in a way similar to the corresponding β-CD·TERB complex. The abrupt increase of ε'' for temperatures higher than 275 K is due to protonic conductivity, which is almost zero in the case of β-CD·TERB·3.8H_2O. The abrupt increase of ε'' versus T becomes smaller as the frequency increases, and disappears completely at frequencies higher than 5 kHz, indicating that the mechanism which is responsible for this absorption has an eigenfrequency smaller than 5 kHz.

Figure 8 shows the phase shift versus temperature plots. It is interesting to note that the temperatures where the minima of the phase shifts are observed are

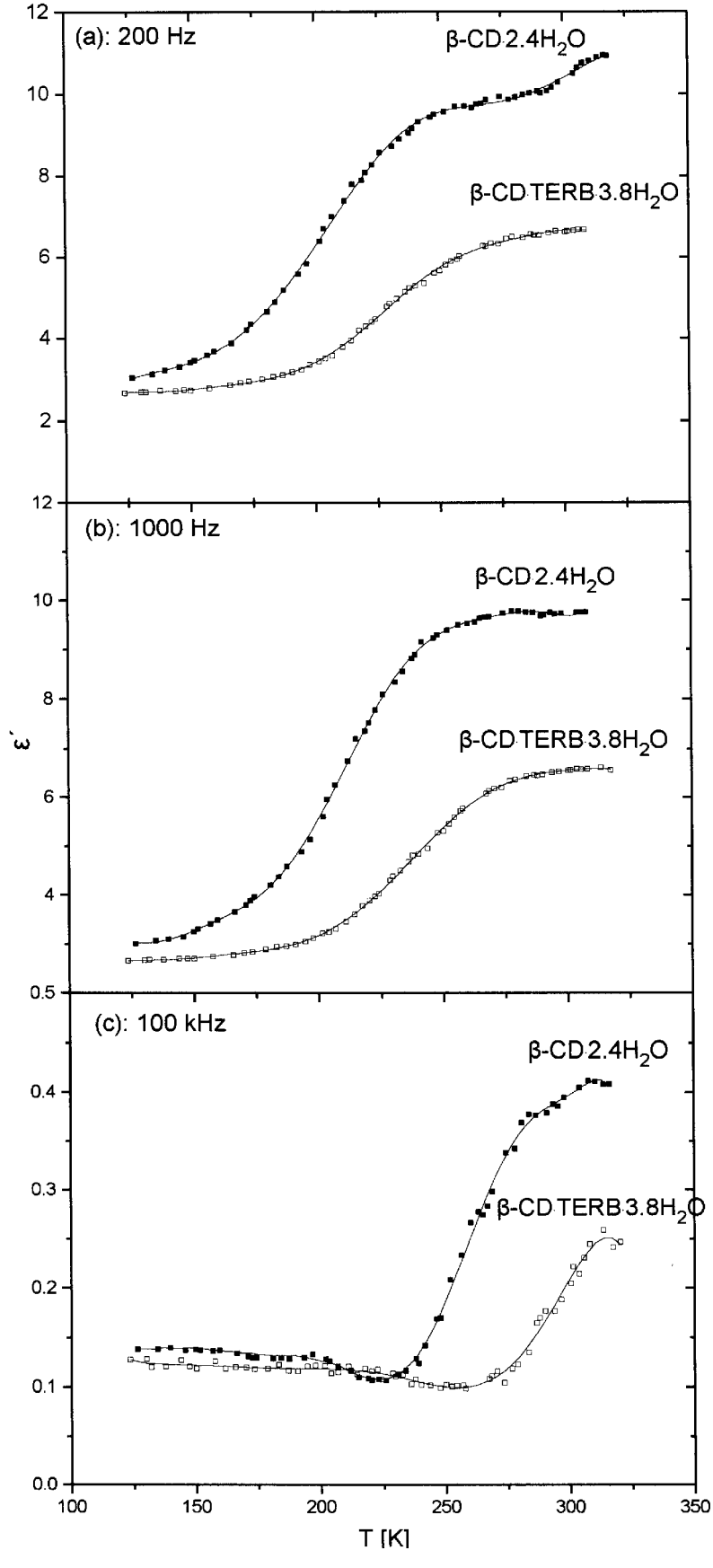

Figure 6. Temperature dependence of ε' for the samples of β-CD · TERB · $3.8H_2O$ and β-CD · $2.4H_2O$ at frequencies (*a*) 200 Hz, (*b*) 1000 Hz and (*c*) 100 kHz.

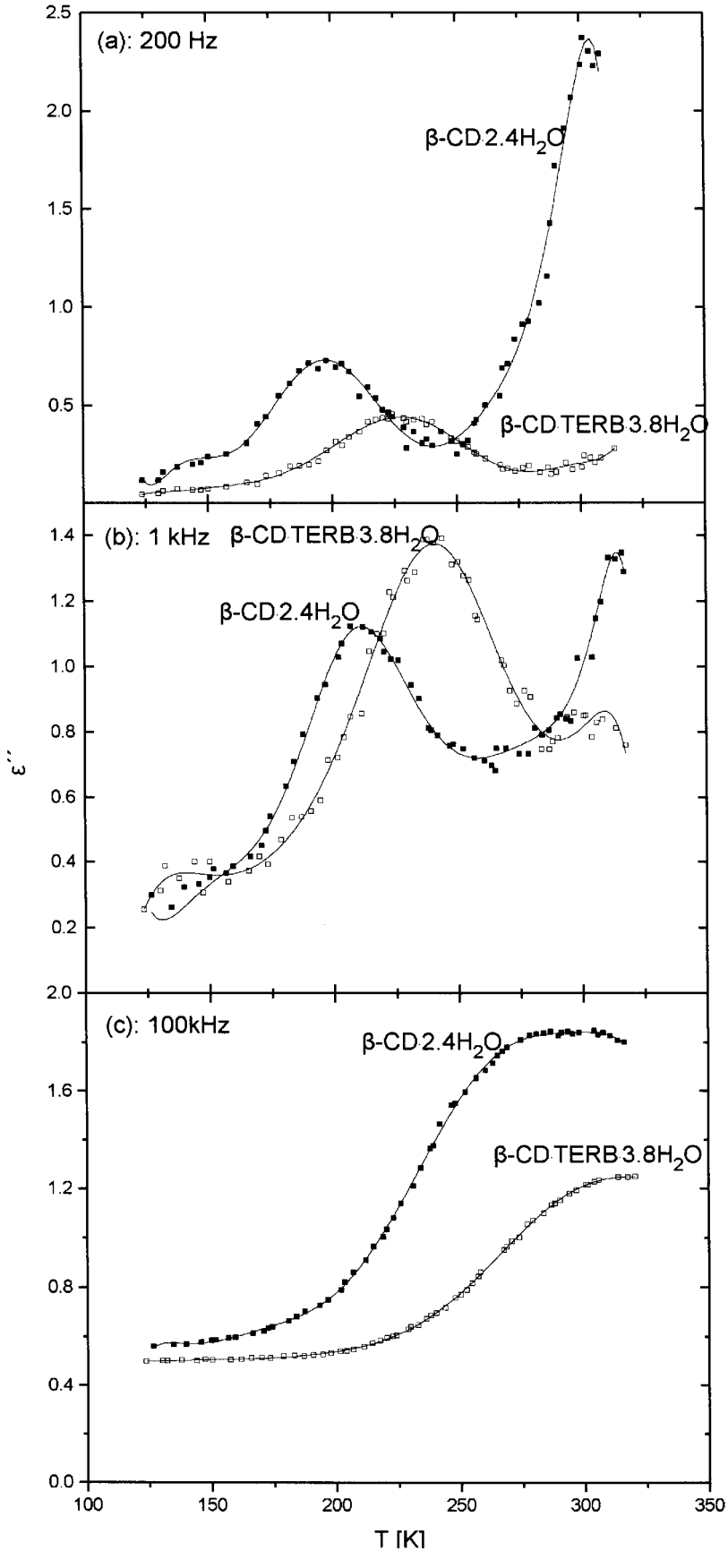

Figure 7. Temperature dependence of ε'' for the samples of β-CD·TERB·3.8H_2O and β-CD·2.4H_2O at frequencies (a) 200 Hz, (b) 1000 Hz, and (c) 100 kHz.

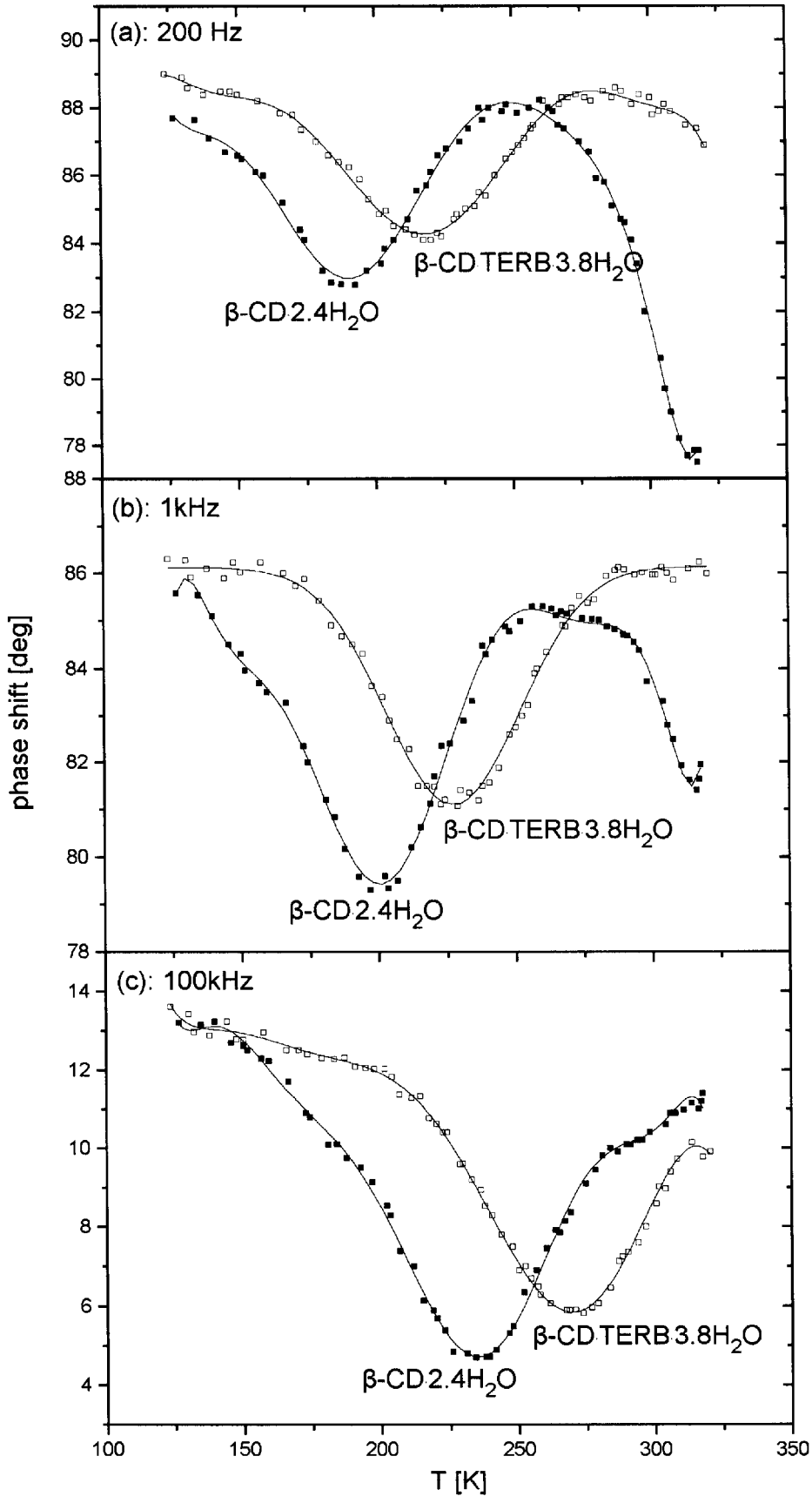

Figure 8. Temperature dependence of phase shift for dried samples of β-CD · TERB · 3.8H_2O and β-CD · 2.4H_2O.

very close to the temperature of the maxima of figure 7. The turning points correspond to a transition attributed to order–disorder. The phase shift (an experimentally measured parameter) versus temperature plots show the temperature of the observed transition even for high frequencies where the ε'' versus temperature curve does not have a maximum. It is interesting to note that dried α-CD did not show any minimum in the phase shift versus temperature plot [16].

3.2.2. *Non-dried samples*

The plots of ε' and ε'' against temperature for the fixed frequencies 200 Hz, 1 kHz, 100 kHz are shown in figures 9 and 10, respectively. The ε' values of β-CD · TERB · $11.2H_2O$ at 200 Hz increase in a double-step fashion from 2.5 at low temperatures to 6.5 at 250 K and then to 11.0 at high temperatures. The ε' values of β-CD · $9.8H_2O$ are almost the same as those of β-CD · TERB · $11.2H_2O$ in the low temperature region, but as the temperature increases they deviate strongly $(\Delta\varepsilon' = 12.5)$. For the fixed frequency of 1 kHz the ε' values vary in the same way $(\Delta\varepsilon' = 7.5)$. For 100 kHz the deviations became very small $(\Delta\varepsilon' = 0.3)$ but their shape which is no longer a double step presents a minimum value at the inflection point of the first step and a maximum value at the inflection point of the second step.

The ε'' versus T curve of β-CD · TERB · $11.2H_2O$, at 200 Hz, is broad-bell shaped with maximum value at 208.0 K and a half-width of ~130 K. This maximum absorption shifts to higher temperatures with increasing frequency up to 1 kHz. Beyond this frequency the bell shaped ε'' versus T curves are transformed to step-like curves similar to the ε' versus T curves. In the case of β-CD · $9.8H_2O$ the maximum value of ε'', at 200 Hz, is located at 188.9 K and shifts to higher temperatures as the frequency increases, in a similar way with that of β-CD · TERB · $11.2H_2O$. An abrupt increase of ε'', due to protonic conductivity, for temperatures higher than 225 K appears in both non-dried samples. In the low temperature range 100–175 K the values of ε' and ε'' are the same for non-dried and dried samples. The phase shift versus temperature curves have the same shapes as those of the dried samples.

4. Discussion

4.1. *Characterization of α and Ω dispersion*

The dependence of ε' and ε'' on frequency (figure 2) in the case of β-CD · TERB · $3.8H_2O$ is described well by Debye relaxation [17] in all the temperatures examined, and the following equations are valid:

$$\varepsilon' = \varepsilon_\infty + \frac{\varepsilon_s - \varepsilon_\infty}{1 + \omega^2\tau^2}, \tag{1}$$

$$\varepsilon'' = \frac{(\varepsilon_s - \varepsilon_\infty)\omega\tau}{1 + \omega^2\tau^2}, \tag{2}$$

$$\varepsilon''_{max} = (\varepsilon_s - \varepsilon_{-\infty})/2. \tag{3}$$

Where ε_s is the static dielectric constant, ε_∞ is the dielectric constant at high frequencies and ε''_{max} is the maximum value of ε''. The validity of the Debye equations is shown from the plots of $\varepsilon''/(\varepsilon' - \varepsilon_\infty)$ against the angular frequency ω, which give straight lines of slope τ passing through the origin, figure 11, according to equation (4):

$$\varepsilon''/(\varepsilon' - \varepsilon_\infty) = \omega\tau. \tag{4}$$

In the case of β-CD · $2.4H_2O$ the system exhibits both dc conductivity (σ) and Debye relaxation, and it is characterized by equations (1) and (5):

$$\varepsilon'' = \frac{(\varepsilon_s - \varepsilon_\infty)\omega\tau}{1 + \omega^2\tau^2} + \frac{\sigma}{\omega\varepsilon_0}, \tag{5}$$

where ε_0 is the vacuum dielectric permittivity. The 'dc contribution' to ε'' is proportional to the specific conductance σ of the system, and inversely proportional to the frequency ω, since the higher the frequency the smaller the available time for cationic motion [18]. If $\omega \ll 1/\tau$ the contribution of conductivity to ε'' will be significant, and this gives rise to the Ω dispersion (figure 3).

X-Ray studies [9] at various humidities have shown that the dehydration of β-CD · $11H_2O$ is due primarily to loss of water from the β-CD cavity through the opening of the primary side. With this in mind, we can explain why there is no proton conduction (Ω dispersion) in the case of samples of dried β-CD · TERB (β-CD · TERB · $3.8H_2O$, figure 2), since the guest 4-*t*-butylbenzyl alcohol molecules have displaced the water molecules from the β-CD cavities and there exist few water molecules in the lattice.

The Debye-type relaxation is valid for only few systems and it refers to (a) the orientation of dipoles in a viscous environment [17], (b) dipole hopping between two states [19, 20] and (c) charge carrier hopping. In the present systems case (b) is the most plausible.

The loss maximum ε''_{max} increases with temperature for both dried and non-dried samples examined, as shown in figure 4. This observation deviates from Debye's theory that requires the maximum amplitude to be independent of temperature (equation (3)). That happens because Debye's theory assumes a fixed number of dipoles of similar energies. In our case the effective number of hopping dipoles increases with temperature

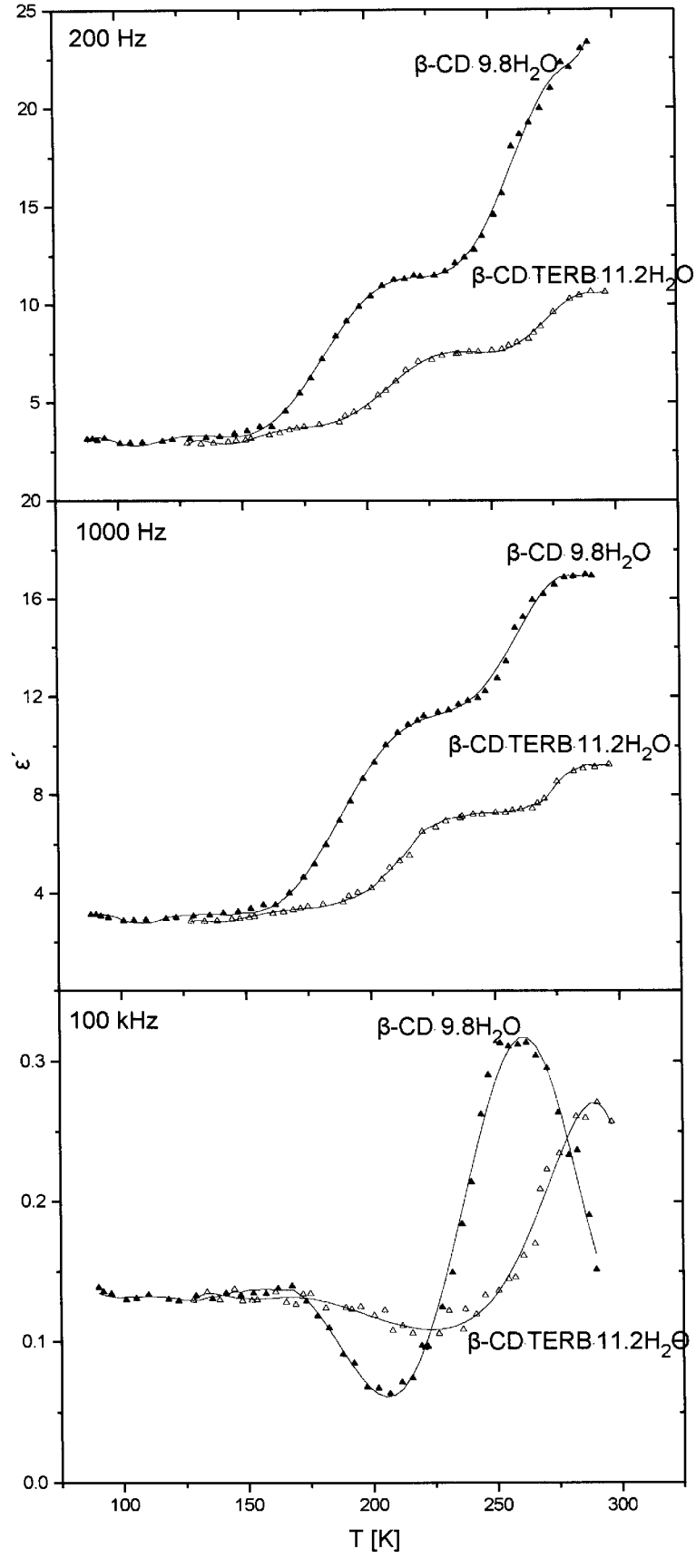

Figure 9. Temperature dependence of ε' for non-dried samples of β-CD·TERB·11.2H_2O and β-CD·9.8H_2O at frequencies (*a*) 200 Hz, (*b*) 1000 Hz, and (*c*) 100 kHz.

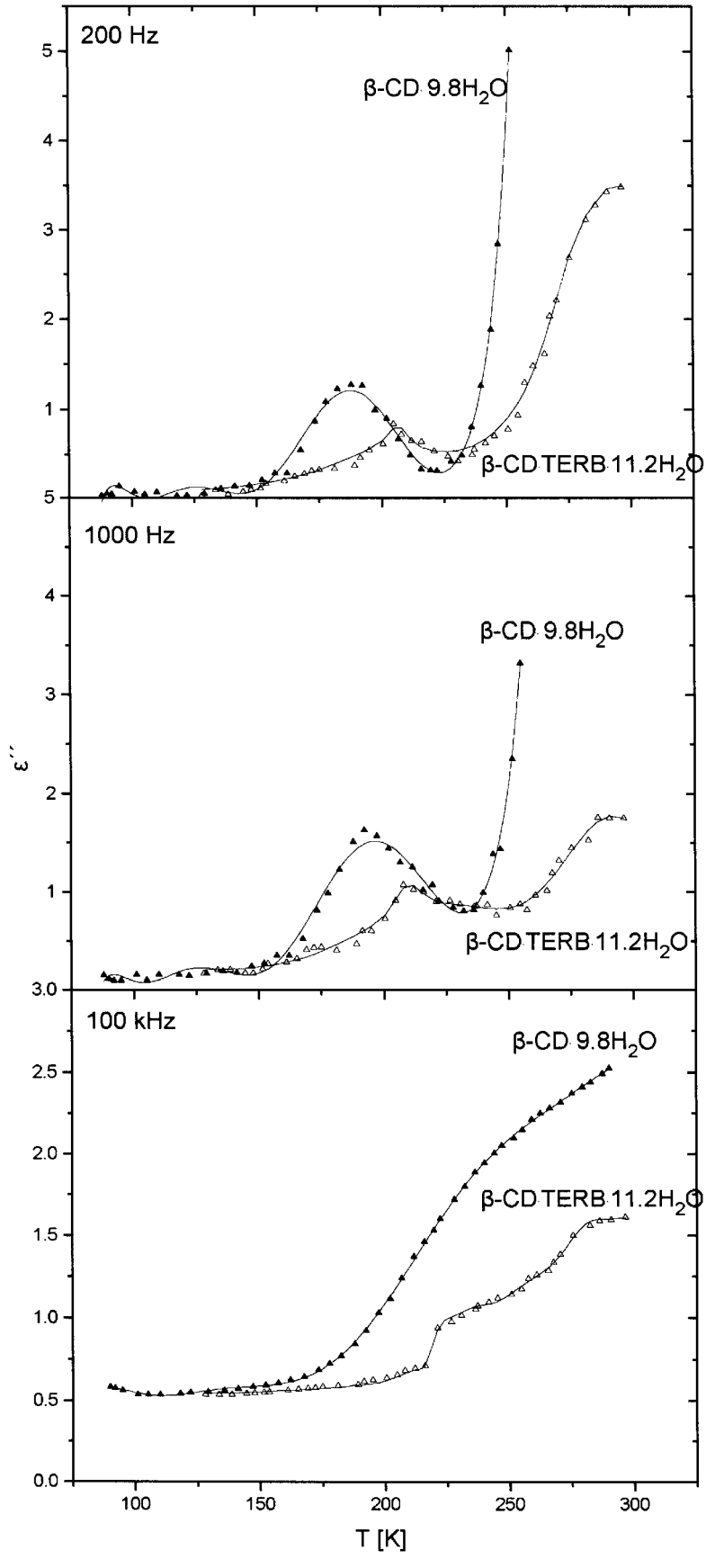

Figure 10. Temperature dependence of ε'' for non-dried samples of β-CD·TERB·11.2H_2O and β-CD·9.8H_2O at frequencies (*a*) 200 Hz, (*b*) 1000 Hz, and (*c*) 100 kHz.

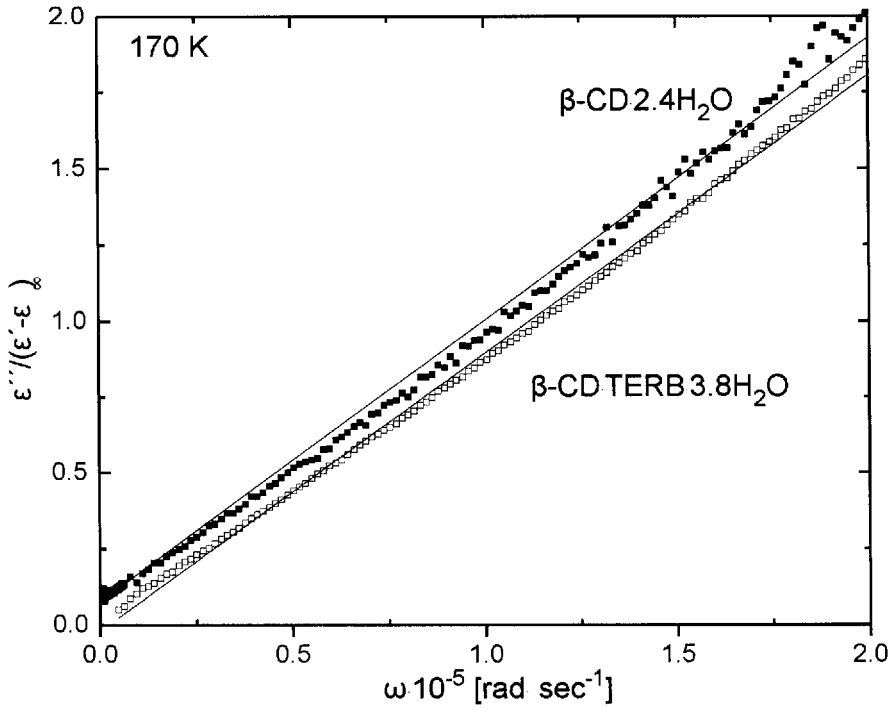

Figure 11. Plots of $\varepsilon''/(\varepsilon' - \varepsilon_\infty)$ against the angular frequency ω for the samples of β-CD·TERB·3.8H_2O and β-CD·2.4H_2O at 170 K.

as the macrocycle's hydroxyl groups and possibly water molecules go from an ordered to a disordered state. Thus there exist more interactions among hydroxyl groups and water molecules. In the case of the non-dried samples the number of hopping dipoles is even higher, because as more water molecules enter the system they are less tightly bound and have a higher probability of being disordered. Therefore, the second stage in the case of non-dried samples can be attributed to the existence of the easily movable water molecules, while the first stage involves strongly bound water molecules.

4.2. *Order–disorder transition and relaxation time*

A flip-flop hydrogen bond arises when the hydrogen atom is disordered over two positions (H_A and H_B) between two oxygen atoms [2, 4]:

$$H_B—O\cdots H_A—O \leftrightarrow O—H_B\cdots O—H_A.$$

A model has been developed [20, 21] in which the molecules have two equilibrium positions, A and B, with opposite dipole directions. Energy of at least E is required for the molecules to turn from one equilibrium position to the other. The A and B positions of figure 12(a) can be considered as the hydrogen positions.

According to rate process theory [18, 22], in the absence of an external electric field the transition probability for a dipole moving between equilibrium states A and B is given by

$$W = v_0 \exp(-E/kT), \tag{6}$$

where v_0 is the vibrational frequency of the hydrogen atoms in the potential well, E is the energy barrier for dipole reorientation, k is the Boltzmann constant and T is the absolute temperature.

For an applied field V, the work done by the field in moving a carrier of charge e by a distance d in the direction of the field is equal to Ved. This work done corresponds to the difference in the potential energy of states A and B (figure 12(b)). The energy barrier to migration in the two directions A → B and B → A is given by $(E - Ved/2)$ and $(E + Ved/2)$, respectively, and hence it is more probable that the dipole turns from state A to state B than vice versa. Therefore, the transition probabilities become

$$W_{A\to B} = v_0 \exp[-(E - eVd/2)/kT], \tag{7}$$

$$W_{B\to A} = v_0 \exp[-(E + eVd/2)/kT]. \tag{8}$$

If $eVd \ll kT$, the net probability P of a dipole hopping from A to B is

$$P = v_0(eVd/kT)\exp(-E/kT). \tag{9}$$

At low temperatures the predominant term of probability P is eVd/kT, which decreases with increasing temperature. The second term, $\exp(-E/kT)$, is the predominant one at high temperatures, and the probability P increases with increasing temperature. Since the relaxation time is inversely proportional to the net probability, the opposite trends should be observed for the

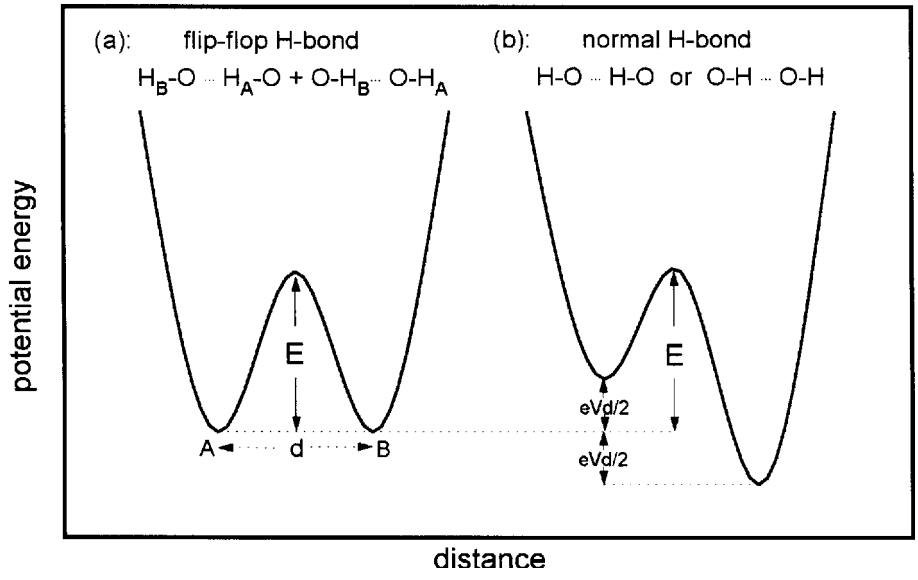

Figure 12. Schematic potential energy diagram showing (*a*) the disordered state (flip-flop hydrogen bond) and (*b*) the normal hydrogen bonded state.

Table 1. Activation energies and transition temperatures of β-CD and the complex β-CD · TERB in dry and non-dry form.

Sample	$T_{transition}$/ K	$E(T < T_{transition})$/ kJ mol^{-1}	$E(T > T_{transition})$/ kJ mol^{-1}
β-CD · 2.4H_2O	215.0	2.41	− 2.23
β-CD · 9.8H_2O	197.3	2.76	− 2.74
β-CD · TERB · 3.8H_2O	246.0	2.39	− 2.18
β-CD · TERB · 11.2H_2O	213.4	2.01	− 2.29

dependence of relaxation time with temperature. It increases at low temperatures and decreases at high temperatures. Therefore, equation (9) explains the τ versus temperature curves (figure 5). The absolute values of τ vary between 8.0 μs and 11.5 μs. These values are in agreement with NMR experiments on hydrated β-CD [23] and with the characteristic Debye correlation time of ~10 μs, at 263 K, related to dipole moment reorientation resulting either from proton transfer or molecular rotation in ice [24].

The transition temperatures listed in table 1 were calculated from the plots of figure 5, τ versus T. Activation energies as calculated from the Arrhenius equation:

$$\tau = \tau_0 \exp(-E/RT) \qquad (10)$$

by plotting $\ln\tau$ against $1/T$ for the linear regions on either side of the transition temperature are listed in table 1 also. These activation energies have small absolute values in the range 1.1–1.7 $kT_{transition}$, and correspond to the heights of the intrinsic barriers shown in figure 12.

The phenomenon of the increase in relaxation time with increasing temperature, implying negative activation enthalpy, has been observed in proteins like lysozyme and collagen [8]. In these cases the activation entropy also was negative, which suggested that the activation processes involve the breaking of a hydrogen bond between the protein and a water molecule and the formation of a more stable hydrogen bond between reoriented water molecules. For the compounds examined we can assume that before the transition temperatures, listed in table 1, a reorientation of the hydrogen bonding around the cyclodextrin molecules is taking place related to the flip-flop hydrogen bonding and to the exothermic and endothermic drifts observed by Hanabata *et al.* [5] in the calorimetric study of β-CD · 11H_2O over the temperature range 120–226 K. The temperatures of the above order–disorder transitions are higher for the dried than for the non-dried samples, which is expected since a large number of less tightly bound water molecules in the non-dried samples facilitates reorientation of hydrogen bonding.

A model of the processes above the transition temperature has been given by a quasielastic neutron scattering experiment on β-CD · 11H_2O [25]. This study showed that dynamic processes which involve formation and breaking of hydrogen bonds and positional fluctuations of water molecules are taking place. A very simple two-site jump model with two different jump distances, 1.5 Å for reorientational jumps of hydroxyl groups and

water molecules and 3 Å for diffusive motions of water molecules enclosed in the β-CD cavity, explain the data very well. At room temperature both types of motion occur with a similar distribution of jump rates extending at least from $2 \times 10^{10}\,s^{-1}$ to $2 \times 10^{11}\,s^{-1}$. This study shows that the diffusive motions can be followed down to at least 240 K.

The present experiments determined relaxation times at the range 8.0–11.5 μs ($\sim 10^5\,s^{-1}$), much lower than the above, which are in the frequency range corresponding to dipole orientation [26] in an external electric field. It is not possible to detect relaxation frequencies higher than $\sim 10^5\,s^{-1}$.

5. Conclusions

The dielectric behaviour of dried and non-dried β-cyclodextrin and its complex with 4-*t*-butylbenzyl alcohol (TERB) are described well by Debye-type relaxation (α dispersion). All systems except dried β-CD·TERB (β-CD·TERB·3.8H_2O) exhibit an additional dc conductivity (Ω dispersion) which is related to proton transport.

In the non-dried systems the temperature dependence of ε' and ε''_{max} exhibits two steps, whereas the dried systems exhibit only one step, coinciding with the low temperature step of the non-dried samples. The low temperature step is caused by the order–disorder transition of the tightly bound water and the hydroxyl groups of β-CD molecule, whereas the other arises from the less tightly bound, easily removable water molecules. The height of the first step is the same in dried and non-dried samples, denoting that the removable water does not contribute to that order–disorder transition. It should be noted that no order–disorder transition temperature was detected in samples of α-cyclodextrins, which do not have flip-flop-type hydrogen bonds, according to a neutron diffraction study [2].

The temperature dependence of ε'' shows a maximum that has been attributed to the order–disorder transition. This maximum vanishes progressively for frequencies higher than 5 kHz, indicating that the mechanism involved has an eigenfrequency smaller than this value. Furthermore the Ω dispersion decreases as the frequency rises, and vanishes above 5 kHz. The absence of Ω dispersion, which is related to proton conduction in the case of β-CD·TERB·3.8H_2O, is not yet clear and currently is under research.

The relaxation time varies exponentially with temperature (in the range 8–12 μs), in a reverse V-like curve, with maximum values at the corresponding order–disorder transition temperatures.

The control of the proton conduction and the mechanism that takes place is of general interest, especially in biological systems.

We thank Dr D. Tsiourvas for his help with the thermogravimetric measurements and the Greek National Research Foundation (I.K.Y.) for the scholarship offered to N. D. Papadimitropoulos.

References

[1] Fujiwara, T., Yamazaki, M., Tomiza, Y., Tokuoka, R., Tomita, K., Matsuo, T., Suga, H., and Saenger, W., 1983, *Nippon Kagaku Kaishi*, **2**, 181.
[2] Betzel, C., Saenger, W., Hingerty, B. E., and Brown, G. M., 1984, *J. Amer. chem. Soc.*, **106**, 7545.
[3] Saenger, W., Betzel, C., Hingerty, B., and Brown, G. M., 1982, *Nature*, **296**, 581.
[4] Zabel, V., Saenger, W., and Mason, S. A., 1986, *J. Amer. chem. Soc.*, **108**, 3664.
[5] Hanabata, H., Matsuo, T., and Suga, H., 1987, *J. Inclusion Phenom.*, **5**, 325.
[6] Pathmanathan, K., Johari, G. P., and Ripmeester, J. A., 1989, *J. phys. Chem.*, **93**, 7491.
[7] Bone, S., and Pethig, R., 1983, *Int J. Quantum Chem. Symp.*, **10**, 133.
[8] Pethig, R., 1992, *Ann. Rev. phys. Chem.*, **43**, 177 and references therein.
[9] Steiner, T., and Koellner, G., 1994, *J. Amer. chem. Soc.*, **116**, 5122.
[10] Mentzafos, D., Mavridis, I. M., Le Bas, G., and Tsoucaris, G., 1991, *Acta Crystallogr.* B, **47**, 746.
[11] Moreira Da Silva, A. M., Steiner, T. H., Saenger, W., Empis, J. M. A., and Teixeira-Dias, J. J. C., 1996, *J. Inclusion Phenom.*, **25**, 21.
[12] Tambouris, K., and Papaioannou, J. C., unpublished.
[13] Hood, W. G., 1994, *wplot version 1.4* (711 Mitchell Conway, AR 72032).
[14] Morgan, H., and Pethig, R., 1984, *Int. J. Quantum Chem. Symp.*, **11**, 209.
[15] Morgan, H., and Pethig, R., 1986, *J. chem. Soc. Faraday Trans* i, **82**, 143.
[16] Papaioannou, J. C., Papadimitropoulos, N. D., and Mavridis, I. M., unpublished.
[17] Debye, P., 1929, *Polar Molecules* (New York: Chemical Catalog Company) p. 77.
[18] Wu, S. L., and Tung, I. C., 1996, *J. Mater. Sci.*, **31**, 2177.
[19] Glasstone, S., Laidler, K. J., and Eyring, H., 1941, *The Theory of Rate Processes* (New York: McGraw-Hill) p. 547.
[20] Fröhlich, H., 1958, *Theory of Dielectrics*, 2nd Edn (Oxford: Clarendon Press) p. 17.
[21] Smyth, C. P., 1955, *Dielectric Behavior and Structure* (New York: McGraw-Hill).
[22] Eyring, H., 1936, *J. chem. Phys.*, **4**, 283.
[23] Usha, M. G., and Wittebort, R. J., 1992, *J. Amer. chem. Soc.*, **114**, 1541.
[24] Wittebort, R. J., Usha, M. G., Ruben, D. J., Wemmer, D. E., and Pines, A., 1988, *J. Amer. chem. Soc.*, **110**, 5668.
[25] Steiner, T., Saenger, W., and Lechner, R. E., 1991, *Molec. Phys.*, **72**, 1211.
[26] West, A. R., 1984, *Solid State Chemistry and Its Applications* (New York: Wiley) p. 536.